Aromatic Hydrocarbon Receptor Polymorphism: Development of New Methods to Correlate Genotype with Phenotype

Andrew Maier, Jana Micka, Kevin Miller, Timothey Denko, Ching-Yi Chang, Daniel W. Nebert, and Alvaro Puga

Center for Environmental Genetics and Department of Environmental Health, University of Cincinnati Medical Center, Cincinnati, OH 45267-0056 USA

Differential CYP1A1 inducibility, reflecting variations in aromatic hydrocarbon receptor (AHR) affinity among inbred mouse strains, is an important determinant of environmental toxicity. We took advantage of the *Ahr* polymorphism in C57BL/6 and DBA/2 mice to develop an oligonucleotide-hybridization screening approach for the rapid identification of DNA sequence differences between *Ahr* alleles. Oligonucleotides containing single-base changes at polymorphic sites were immobilized on a solid support and hybridized with C57BL/6 or DBA/2 AHR cDNA radiolabeled probes. The observed hybridization patterns demonstrate that this approach can be used to detect nucleotide differences in the *Ahr* coding region with very high accuracy. In parallel experiments, we used a yeast two-hybrid system to assess phenotypic differences in AHR function. AHR activation, as measured by β-galactosidase reporter activity in *Saccharomyces cerevisiae* strain SFY526, was determined following treatment with varying doses of the AHR ligand β-naphthoflavone (BNF). We found that the C57BL/6 AHR has about a 15-fold higher affinity for BNF than the DBA/2 AHR, in much better agreement with results reported for whole-animal studies than the values observed by *in vitro* ligand-binding assays. Using C57BL/6 and DBA/2 AHR chimeric proteins, we also confirmed the previously reported observation that an A375V change is principally responsible for the high- to low-affinity AHR phenotype. There has been no straightforward method to reliably and reproducibly phenotype large numbers of humans for CYP1A1 inducibility or AHR affinity. Screening human AHR cDNAs by oligonucleotide-hybridization and yeast two-hybrid methodologies will be invaluable for the rapid and unequivocal determination of changes in DNA sequence and receptor–ligand affinities associated with human *AHR* polymorphisms. *Key words*: aromatic hydrocarbon (Ah) receptor, mouse *Ahr* gene polymorphism, oligonucleotide hybridization, yeast two-hybrid system, β-naphthoflavone. *Environ Health Perspect* 106:421–426 (1998). [Online 12 June 1998]
http://ehpnet1.niehs.nih.gov/docs/1998/106p421-426maier/abstract.html

One of the most challenging questions facing environmental health research today is the identification of genotype changes associated with phenotypes of increased resistance or susceptibility to toxic environmental agents. Environmental pollutants generate varying degrees of response in an exposed population, often due to polymorphisms in the genes controlling the molecular mechanisms of the toxic response. For example, a clear genetic component exists in the susceptibility of mouse strains to many halogenated aromatic hydrocarbons (HAHs) and nonhalogenated polycyclic aromatic hydrocarbons (PAHs), such as 2,3,7,8-tetrachlorodibenzo-*p*-dioxin (dioxin) and benzo(*a*)pyrene (BaP), respectively. These two environmental compounds exhibit a high degree of toxicity. BaP is a potent carcinogen in animals and a suspected carcinogen in humans (*1*). Dioxin is associated with a variety of systemic effects, including immunosuppression, cleft palate, and tumor promotion in animals, and chloracne, immunosuppression, and possibly cancer and heart disease in humans (*2,3*). There is no instance known so far in which dioxin or BaP toxicity or carcinogenesis in laboratory animals is not mediated by the aromatic hydrocarbon receptor (AHR), a transcriptional regulator of xenobiotic-metabolizing enzymes encoded by the mammalian *AHR* gene (*4,5*).

A mouse *Ahr* polymorphism is known to be responsible for the variation in susceptibility to PAHs and HAHs (*6–8*). Four distinct mouse *Ahr* alleles have now been characterized, each encoding receptor proteins with differing ligand affinities (*9*). The $Ahr^{b\text{-}1}$, $Ahr^{b\text{-}2}$, and $Ahr^{b\text{-}3}$ alleles code for AHRs with higher affinity than the AHR encoded by the Ahr^{d} allele (*9*). The $Ahr^{b\text{-}1}$ allele occurs in C57, C58, and MA/My inbred strains; the $Ahr^{b\text{-}2}$ allele is carried by the C3H, BALB/cBy, and A inbred strains; the $Ahr^{b\text{-}3}$ allele exists in *Mus caroli*, *Mus spretus*, and MOLF/Ei; and the Ahr^{d} allele occurs in AKR, DBA/2, and 129 strains (*9*).

Ahr nucleotide differences, and corresponding AHR amino-acid changes between the C57BL/6 (B6) and DBA/2 (D2) mouse strains that carry the $Ahr^{b\text{-}1}$ and Ahr^{d} alleles, respectively, have been studied extensively (*9–15*). An A375V change has been reported to confer most of the observed phenotypic differences between B6 and D2 (*15*). With hepatic cytosol from B6 and D2 mice, ligand–affinity differences were found to range between 4- and 10-fold for the B6 and D2 AHRs (*16–18*), whereas ligand–affinity differences range between 2- and 6-fold for the B6 and D2 AHRs when cDNA-expressed AHRs are studied (*9,15*). These *in vitro* ligand-binding assays appear not to accurately reflect the *in vivo* variability in this polymorphism, however, because the B6–D2 differences in hepatic aryl hydrocarbon hydroxylase (CYP1A1) inducibility in the intact mouse are much larger—in the order of 15- to 30-fold (*6–8,19*).

Many of the toxic effects of AHR ligands observed in mice also occur in exposed human populations, in which a large amount of interindividual variability is seen; however, a DNA-based explanation of the human *AHR* polymorphism is still to be determined. CYP1A1 inducibility varies by more than 30-fold in humans (*20–23*), and Scatchard plot analyses of 106 human placental samples have shown a >35-fold difference in AHR affinity between the highest and lowest phenotype (*24,25*), yet there has not been any direct correlation established between the degree of CYP1A1 inducibility and the variation in AHR affinity in humans (*26–29*). No nucleotide or amino acid change in the human AHR has been unequivocally associated with ligand variability. Substitution of alanine for valine at position 381 (equivalent to position 375 in the mouse) was shown to increase ligand affinity several-fold in an *in vitro* cDNA-expression binding assay (*15*); however, the human AHR protein from the HepG2 and A431 cell lines, as well as from at least eight individuals, contains valine at position 381 in all cases (*15,22,26–29*). Another

Address correspondence to A. Puga, Department of Environmental Health, Center for Environmental Genetics and Department of Environmental Health, University of Cincinnati Medical Center, 123 E. Shields Street, Cincinnati, OH 45267-0056 USA.

We thank Noll Hankinson for the gift of pCDNAneo/ARNT encoding the full-length mouse ARNT cDNA, and Sohaib Khan and Jun Ma for advice on the yeast two-hybrid methodology. We also thank Ralph Buncher and Peter Gartside for help with statistical analysis of our data.

This work was supported by NIEHS grants ES06273, P30 ES06096, ES06811, and ES07250. A.M. was supported in part by a U.S. EPA STAR Fellowship Grant; J. M. and T. D. were supported by an American Heart Association Fellowship Grant; and C.-Y.C. was supported by a predoctoral fellowship from the Pharmaceuticals Research and Manufacturers of America Foundation.

Received 9 January 1998; accepted 16 March 1998.

nucleotide change in exon 2 of the human *AHR* gene has been reported (*29*), but no phenotypic changes associated with this polymorphism were examined.

Progress in correlating any human *AHR* genotype with variations in the AHR phenotype has been hindered by the lack of efficient methods for screening large numbers of individuals. Recently, reverse transcriptase-polymerase chain reaction (RT-PCR) has been successful for rapidly sequencing portions of the *AHR* gene (*22,29*), but this approach has been limited to small groups of individuals and may be too cumbersome for identification of nucleotide changes in large populations. Approaches that rely on oligonucleotide hybridization (*30*), however, may provide a solution to this problem, particularly in light of the recent advances in DNA chip technology (*31*).

Detection of nucleotide differences must be coupled to the analysis of resulting functional changes in order to assess the relevance of any given polymorphism to environmentally related disease. In the case of the AHR, the use of mammalian tissue culture systems for this purpose has clearly proven to be unreliable. For example, expression of exogenous AHR in AHR-deficient CV-1 African green monkey kidney epithelial cells and mouse hepatoma *c35* cells results in high basal CYP1A1 activity and low inducibility (*32–34*), possibly due to the presence of an endogenous AHR ligand (*35*); therefore, the expression of exogenous AHR in cell culture would not be useful for phenotypic characterization of the human AHR. A widely used method for the phenotypic analysis of human AHR function has been the mitogen-activated lymphocyte culture assay for CYP1A1 induction (*36*). Implementation of this method is not trivial, with many laboratories experiencing difficulties in reproducibility (*37,38*). These findings underscore the importance of developing a reliable, efficient, and noninvasive test to determine AHR phenotype in large human populations.

The yeast *Saccharomyces cerevisiae* may provide the means for such a quantitative phenotyping test; in contrast to AHR-deficient mammalian cell lines, expression of exogenous AHR in yeast generates a highly sensitive detection system for the analysis of AHR activation (*34,39–41*). In this report, we have used the well-characterized *Ahr* polymorphism between B6 and D2 mice to optimize an oligonucleotide-hybridization screening approach for the identification of *Ahr* nucleotide changes and to develop a yeast two-hybrid approach for the functional analysis of the corresponding AHR protein.

Materials and Methods

Sequencing by hybridization. Twelve sets of four 21-residue oligonucleotides (Table 1), for a total of 48 target oligonucleotides, were commercially synthesized (Bio-Synthesis, Inc., Lewisville, TX) for hybridization experiments. Each set corresponded to 1 of the 11 sites at which the Ahr^{b-1} and Ahr^{d} alleles differed, plus 1 control site at which both alleles were identical. The four oligonucleotides in a set differed only by the middle 11th residue, which contained A, C, G, or T. For each set, one oligonucleotide matched Ahr^{b-1}, another matched Ahr^{d}, and the other two matched neither.

The sequences and theoretical dissociation temperatures of 23 of the 48 oligonucleotides are shown in Table 1. Five of the 11 polymorphic sites encode amino acid sequence changes. Oligonucleotides were transferred to a Nytran membrane (Schleicher & Schuell, Keene, NH) using a slot-blotting apparatus (Bio-Rad, Richmond, CA). Each oligonucleotide (1 µg) was applied to a slot by filtration under vacuum, washed with 0.5 M sodium phosphate buffer (pH 7.0), and UV cross-linked to the membrane. Membranes were hybridized with B6, D2, or each of eight chimeric AHR cDNA probes (containing combinations of the polymorphic sites from the Ahr^{b-1} and Ahr^{d} alleles). The chimeric cDNAs were constructed using standard recombinant DNA techniques (*12,35*), and encode the amino acid changes shown in Figure 1. cDNA probes were labeled with [^{32}P]dCTP (Amersham, Arlington Heights, IL) by nick translation (Gibco-BRL, Inc., Rockville, MD). Membranes were prehybridized in a buffer containing 6X SSC (0.9 M NaCl, 0.09 M sodium citrate), 1% sodium dodecylsulfate, and 100 µg denatured calf thymus DNA per milliliter. Hybridizations were carried out in the same buffer, with the addition of 1×10^6 dpm/ml [^{32}P]-labeled probe. Following overnight hybridization at temperatures ranging from 46°C to 60°C,

Table 1. Oligonucleotides for the detection of mouse *Ahr* polymorphism

NT	*Ahr* Allele	Oligonucleotide sequence	T_D °C	AA
2038	*b-1*	TACATCATCG**C**CACTCAGAGA	62	Alanine
	d	T	60	Valine
2198	*b-1/d*	CAATACGCACCAAAAGCAACA	60	Proline
2303	*b-1*	CCATCTATCT**G**TGTCCTCCTT	62	Leucine
	d	A	60	Leucine
2326	*b-1*	AGCCCTGCGC**T**GTTAGACAGC	68	Leucine
	d	C	70	Proline
2512	*b-1*	GACTTGTACA**G**CATCATGAGG	62	Serine
	d	A	60	Asparagine
2594	*b-1*	ACTCCACCGC**T**GCTGGTGAGG	70	Alanine
	d	C	72	Alanine
2679	*b-1*	TTCAACTTTG**C**TGAACTCGGC	62	Leucine
	d	A	60	Methionine
2687	*b-1*	TGCTGAACTC**G**GCTTGCCAGC	68	Serine
	d	C	68	Serine
2747	*b-1*	AGCGCCTGCA**A**CTAGAGCAAC	66	Glutamine
	d	T	66	Glutamine
3098	*b-1*	ATTTTGAACC**G**TCCCTGCATC	62	Proline
	d	A	60	Proline
3330	*b-1*	GGTGCAGAGT**T**GAGGTGTTTT	62	Opal
	d	C	64	Arginine
3336	*b-1*	GAGTTGAGGT**G**TTTTCAATGA	58	–
	d	A	56	Isoleucine

Abbreviations: NT, nucleotide position within the cDNA sequence (*12*); T_D, theoretical dissociation temperature of the perfect hybrid calculated from the sequence; AA, amino acid encoded by the corresponding codon at the polymorphic site. Oligonucleotides (21-mers) were synthesized for 10 polymorphic sites in the coding region of the mouse *Ahr* gene, 1 polymorphic site outside the coding region, and 1 control site of sequence identity between C57BL/6 and DBA/2. The sequence shown corresponds to the Ahr^{b-1} allele. In each case, the middle nucleotide (in bold) was replaced by each of the other three nucleotides, one of which matches that of the Ah^{d} allele (shown below each sequence); the other two oligonucleotides of each set are not shown. At positions 2679, 2687, 3330, and 3336—due to the proximity of two Ahr^{b-1}/Ahr^{d} polymorphic sites—the Ahr^{d} consensus oligonucleotides contain an additional nucleotide change.

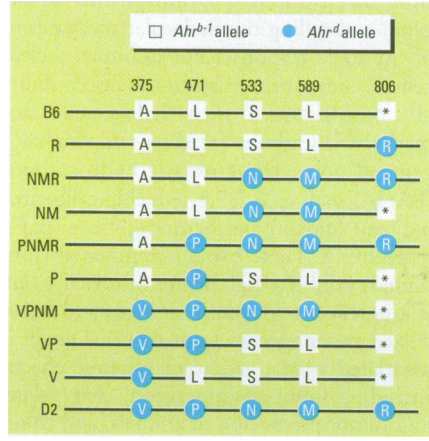

Figure 1. Schematic structure of C57BL/6 (B6), DBA/2 (D2), and chimeric B6–D2 AHR constructs used in these studies. Abbreviations: A, alanine; V, valine; L, leucine; P, proline; S, serine; N, glutamic acid; M, methionine; R, arginine.
*Represents the *opal* termination codon.

membranes were washed at the hybridization temperature in 6X SSC, 0.1% sodium dodecylsulfate, and exposed to x-ray film. Hybridization intensities were quantified by phosphorimaging in a Storm 860 (Molecular Dynamics).

Yeast plasmid constructs and yeast transformation. The B6, D2, and eight chimeric AHR cDNAs, cloned in the eukaryotic expression vector pCDNAI/ Amp (*35*), were excised from this vector and cloned into the *trp*$^+$ yeast expression vector pGBT9 (ClonTech, Palo Alto, CA) in-frame with the DNA binding domain of GAL4, resulting in each of 10 different pGBT9AHR plasmids. The AHR nuclear translocator (ARNT) full-length cDNA was excised from pCDNAneo/ ARNT and cloned into the *leu*$^+$ yeast vector pGAD424 (ClonTech) in-frame with the GAL4 transactivation domain, resulting in plasmid pGAD424ARNT. *S. cerevisiae* strain SFY526 (*leu*$^-$, *trp*$^-$) was grown in YEPD medium (10 g/l yeast extract, 2 g/l peptone, 20 g/l dextrose, 253 mg/l adenine, 133 mg/l uracil) and transformed by electroporation with pGAD424ARNT and plated on yeast minimal medium (1 M sorbitol, 1.7 g yeast nitrogen base/l, 1 g/l ammonium sulfate, 10 g/l succinic acid, 6 g/l NaOH, 20 g/l dextrose, 2% (w/v) agar, and a cocktail of essential amino acids minus leucine). After incubation at 30°C, individual colonies were grown in liquid medium (same medium as above but without sorbitol or agar), transformed with each of the pGBT9AHR plasmids by electroporation, and plated on minimal medium minus leucine and tryptophan. Several individual colonies from these plates were then used for the AHR activation studies.

β–Galactosidase assays. Minimal medium minus leucine and tryptophan was inoculated with individual yeast colonies and grown overnight at 30°C to saturation. Dioxin, β-naphthoflavone (BNF), or BaP (dissolved in dimethylsulfoxide) was then added to fresh medium to final concentrations ranging from 10^{-10} to 10^{-5} M, and the medium was inoculated with an aliquot of the saturated yeast cultures to an OD_{600} (optical density) ranging between 0.05 and 0.2. Control cultures were treated with an equivalent amount of dimethylsulfoxide vehicle. All cultures were grown 8–12 hr and harvested by centrifugation. The cells were washed in a buffer (containing 100 mM HEPES, 150 mM NaCl, 4.5 mM hemimagnesium salt of L-aspartate, 10 mg/ml bovine serum albumin, and 0.05% Tween 20) and lysed by freezing in liquid nitrogen.

β-galactosidase activity was determined by adding 2.2 mM chlorophenol red-β-D-galactopyranoside (CPRG) and incubating the reaction for varying periods of time at room temperature. The colorimetric reaction was stopped by addition of $ZnCl_2$ to a final concentration of 1 mM; β-galactosidase activity was assessed by measuring the absorbance at 578 nm and calculated using the equation:

β-galactosidase activity = $(1{,}000 \times A_{578})/[A_{600} \times \text{cell volume (ml)} \times \text{time (min)}]$.

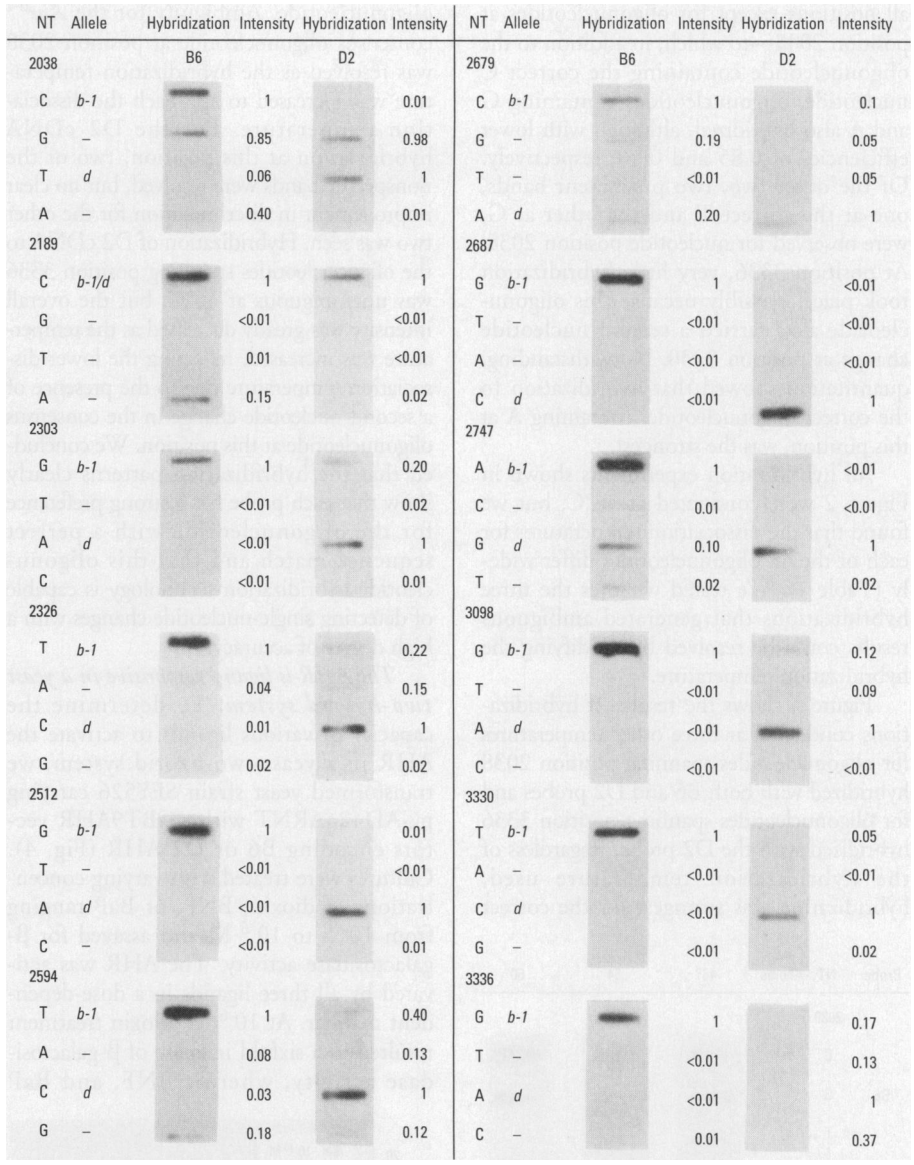

Figure 2. Hybridization of C57BL/6 (B6) and DBA/2 (D2) cDNA probes to oligonucleotide arrays spanning all polymorphic sites in the Ahr^{b-1} and Ahr^{d} alleles. The hybridization temperature was 56°C. The allele, the nucleotide (NT), and its position in the AHR cDNA are indicated adjacent to a representative example of a hybridization experiment. Hybridization intensities were quantitated for all probes, and the mean values relative to the maximum for each oligonucleotide in a set are shown.

Results

Detection of single Ahr nucleotide changes by oligonucleotide hybridization. To test whether the oligonucleotide-hybridization screening approach could be used to identify nucleotide changes reflecting amino acid differences, we hybridized B6, D2, and chimeric AHR cDNA probes to an oligonucleotide array containing single-base substitutions at all mouse *Ahr* polymorphic sites, plus the one control invariant site. Representative hybridization results are shown in Figure 2 for each of the 12 sets of four oligonucleotides. The relative hybridization intensities of all the probes were calculated for each oligonucleotide array position, and the means for a given nucleotide position are shown adjacent to the corresponding slot. In all cases, hybridization was strongest with the correct oligonucleotide, although we detected varying degrees of hybridization to the other three oligonucleotides. Hybridization to Ahr^{b-1} sequences by 11 of the 12 B6 probes and hybridization to Ahr^{d} sequences by 10 of the 12 D2 probes occurred with the highest degree of specificity. Nonspecific binding was less than 19% of maximum for

all positions except for oligonucleotides at position 2038—to which, in addition to the oligonucleotide containing the correct C nucleotide, oligonucleotides containing G and A also hybridized, although with lower efficiencies of 0.85 and 0.40, respectively. Of the other two, two prominent bands, one at the correct T and the other at G, were observed for nucleotide position 2038. At position 3336, very little hybridization took place, possibly because this oligonucleotide also carried a second nucleotide change at position 3330. Notwithstanding, quantitation showed that hybridization to the correct oligonucleotide, containing A at this position, was the strongest.

All hybridization experiments shown in Figure 2 were conducted at 56°C, but we found that the dissociation temperatures for each of the 48 oligonucleotides differ widely (Table 1). We tested whether the three hybridizations that generated ambiguous results could be resolved by modifying the hybridization temperature.

Figure 3 shows the results of hybridizations conducted at three other temperatures for oligonucleotides spanning position 2038 hybridized with both B6 and D2 probes and for oligonucleotides spanning position 3336 hybridized with the D2 probe. Regardless of the hybridization temperature used, hybridization was strongest for the correct oligonucleotide. Ambiguity for the Ahr^{b-1} consensus oligonucleotide at position 2038 was resolved as the hybridization temperature was increased to approach the dissociation temperature. For the D2 cDNA hybridization at this position, two of the nonspecific bands were resolved, but no clear improvement in discrimination for the other two was seen. Hybridization of D2 cDNA to the oligonucleotides spanning position 3336 was unambiguous at 46°C, but the overall intensity was greatly decreased as the temperature was increased, reflecting the lower dissociation temperature due to the presence of a second nucleotide change in the consensus oligonucleotide at this position. We concluded that the hybridization patterns clearly show that each probe has a strong preference for the oligonucleotide with a perfect sequence match and that this oligonucleotide-hybridization technology is capable of detecting single-nucleotide changes with a high degree of accuracy.

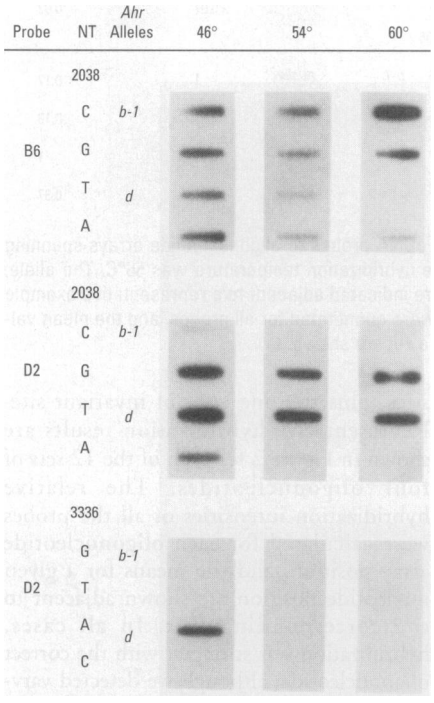

Figure 3. Resolution of hybridization ambiguities by changing the hybridization temperature. Oligonucleotides spanning positions 2038 or 3336 were hybridized at 46°C, 54°C, and 60°C to the C57BL/6 (B6) and DBA/2 (D2) cDNA probes. Position, alleles, and hybridization temperatures are indicated.

The AHR is ligand responsive in a yeast two-hybrid system. To determine the capacity of various ligands to activate the AHR in a yeast two-hybrid system, we transformed yeast strain SFY526 carrying pGAD424ARNT with pGBT9AHR vectors encoding B6 or D2 AHR (Fig. 4). Cultures were treated with varying concentrations of dioxin, BNF, or BaP ranging from 10^{-10} to 10^{-6} M and assayed for β-galactosidase activity. The AHR was activated by all three ligands in a dose-dependent manner. At 10^{-6} M, dioxin treatment resulted in a sixfold increase of β-galactosidase activity, whereas BNF, and BaP caused 16- and 19-fold increases, respectively. At any ligand concentration tested, we found that activation of the B6 AHR was greater than that of the D2 AHR, regardless of which ligand was used (data not shown). The low levels of induction by dioxin at doses 1,000-fold higher than those needed in mammalian cells are probably due to low permeability of yeast cells for very hydrophobic compounds. These results confirm work by others (*34,39–41*), demonstrating that a yeast two-hybrid system can be used to assess ligand-dependent activation of the AHR.

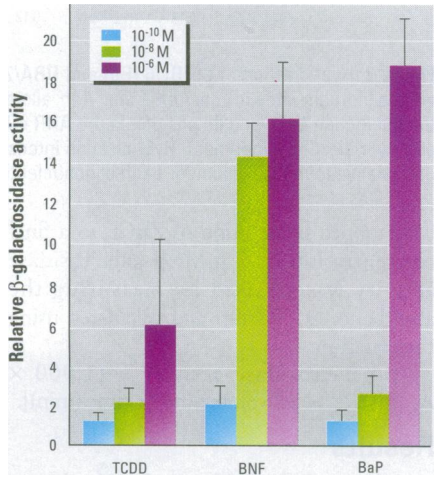

Figure 4. β-galactosidase activity following treatment of yeast with three aromatic hydrocarbon receptor ligands at three concentrations. Abbreviations: TCDD, 2,3,7,8-tetrachlorodibenzo-*p*-dioxin; BNF, β-naphthoflavone; BaP, benzo(*a*)-pyrene. Assay results are reported as fold increases over dimethylsulfoxide-treated controls. Each bar represents the mean ± standard deviation of three samples.

Quantitation of AHR ligand affinity in the yeast two-hybrid system. The observation that the AHR is ligand responsive in yeast (Fig. 4) led us to test whether the yeast two-hybrid assay could be used to assess functional differences in AHR phenotype, i.e. variability in ligand affinity. Using doses of BNF ranging from 10^{-10} to 10^{-5} M, we found that BNF activates the B6 AHR at a dose approximately 15-fold lower than the D2 AHR (Fig. 5A).

To identify amino acid changes responsible for this difference in induction levels, dose–response experiments were conducted with the chimeric AHR constructs (illustrated in Fig. 1). We found a clear bimodality in dose–response curves of the different chimeric AHR proteins (Fig. 5B). Regardless of other changes, all chimeras carrying alanine (Ala)-375 responded in a fashion similar to that of the B6 receptor, whereas chimeras containing valine (Val)-375 responded like the D2 receptor. In addition, plateau values at the higher doses were 1.5- to 2-fold higher for the B6-like chimeras (data not shown).

Dose–response data were fitted to a four-parameter function to estimate the dose capable of generating the half-maximal activation of the β-galactosidase reporter gene (EC_{50}). Table 2 presents the EC_{50} values for B6, D2, and all eight AHR chimeras. AHR proteins carrying Val-375 were found to exhibit 14- to 24-fold higher EC_{50} values than AHR proteins containing Ala-375.

Discussion

We have shown in this report that oligonucleotide hybridization screening can be effectively used to identify mouse *Ahr* nucleotide differences with a high degree of success and reliability. From an array of 48 oligonucleotides containing individual base substitutions at 11 polymorphic sites, specific hybridization was evident for 11 of the 12 Ahr^{b-1} allele sites and 10 of 12 Ahr^{d} allele sites. We have also shown that hybridization to the incorrect oligonucleotide for the other three sites occurred—to varying degrees, causing less-than-definitive results—for two reasons:

use of suboptimal hybridization temperature and close proximity of two polymorphic sites.

Our results demonstrate the power of this method to identify sequence polymorphisms without the need for DNA sequencing. Although this is the first report of the application of oligonucleotide hybridization screening of the *Ahr* gene, this approach has been used successfully to detect polymorphic alleles of several genes, including β^S-globin, *HLA-A*, *BRCA1*, and β-thalassemia (*42–46*).

We envision the application of modifications of this method (e.g., DNA chip technology) for the rapid and unequivocal screening of the human *AHR* gene polymorphism in a large number of individuals. The complete 2,547-nucleotide coding sequence of the human AHR cDNA could be represented in an array of 849 21-mer sequential oligonucleotides, each beginning three nucleotides after the previous one. Any polymorphism, detected by absence of hybridization to the test probe, would be present in seven (21/3) sequential oligonucleotides. Inclusion of control and test probes labeled with different fluorescent dyes in the same hybridization reaction would provide a rapid and efficient means of detecting possible polymorphisms. Dozens of samples could be processed in a single day. Resolution of ambiguities and determination of the actual nucleotide present at a polymorphic site could then be determined simply by direct sequencing of the corresponding short stretch of DNA, thus greatly decreasing the cost and time needed for screening a large number of samples.

We also have also demonstrated in this report the usefulness of a yeast two-hybrid assay to quantitate the mouse AHR phenotype, i.e., its ligand affinity. The phenotypic variation, ranging from 15- to 30-fold differences, between the B6 and D2 AHR proteins in the intact animal was shown to be accurately reflected in the yeast two-hybrid system.

As measured by β-galactosidase reporter activity in this assay, the EC_{50} for BNF is about 15-fold lower for B6 than D2, in good agreement with B6–D2 differences in CYP1A1 inducibility in the intact animal, and two to four times greater than B6–D2 differences reported in *in vitro* ligand-binding studies (*9,15*). In addition, using chimeric AHRs, we were able to verify in this biological system the importance of the A375V change in generating the low-affinity phenotype.

The yeast two-hybrid system thus appears to represent more faithfully the biological difference in CYP1A1 inducibility phenotype than *in vitro* ligand-binding assays. *In vitro*, the low-affinity forms of the AHR require stabilization by molybdate (*17*), whereas in the yeast system this artificial stabilization of the AHR is not required, perhaps providing a more accurate physiological model of AHR function. In addition, different AHR phenotypes might reflect aspects of AHR activation other than ligand binding, such as translocation to the nucleus or dimerization with ARNT (*5*) that are not evaluated in the *in vitro* ligand-binding assays.

The existence of a human *AHR* polymorphism to explain the observed variability in CYP1A1 inducibility (*20–22*) and AHR affinity (*24–26*) has been hypothesized for many years; however, conclusive evidence to demonstrate this putative polymorphism is lacking (*23,37,38*). Among the B6, D2, C3H, and *Mus spretus* mouse lines, there are 12 AHR amino acid differences (*9–15*). While most amino acid changes were shown

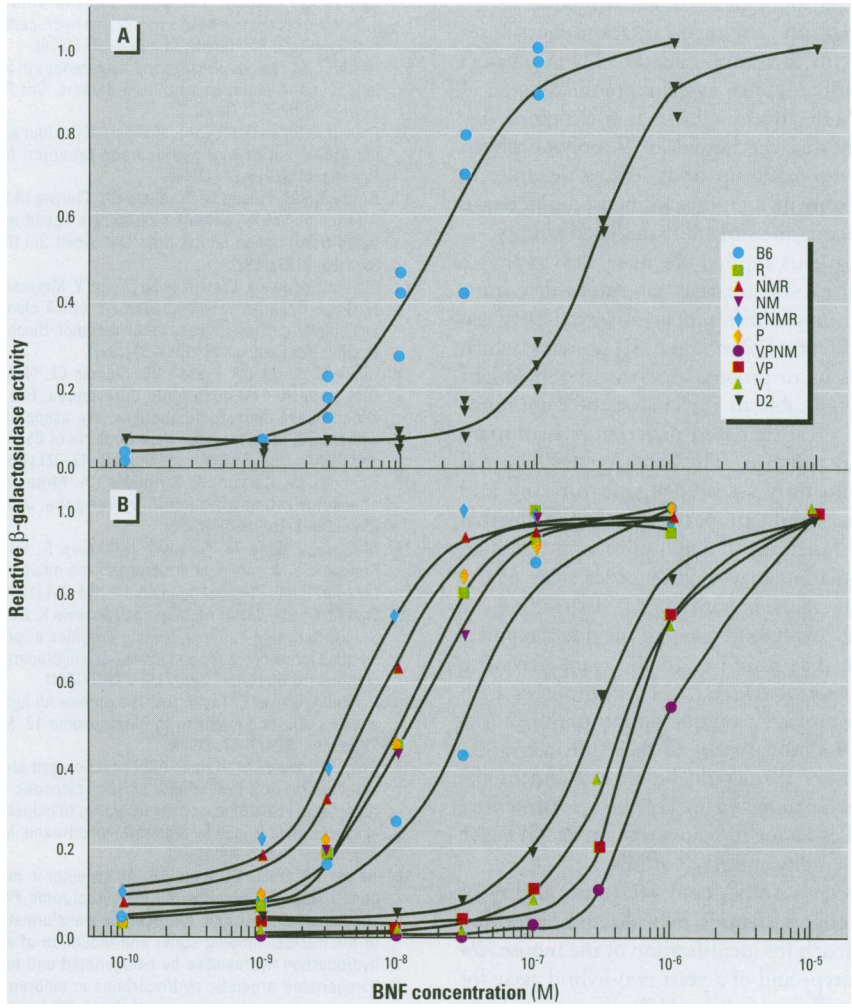

Figure 5. BNF dose–response curves for variant AHR proteins expressed in yeast. Abbreviations: BNF, β-naphthoflavone; AHR, aromatic hydrocarbon receptor; B6, C57BL/6; D2, DBA/2; max, maximum; min, minimum; i, inflection point; s, slope factor. (A) BNF dose–response curves of β-galactosidase activity, representing BNF activation of the B6 and the D2 AHR. All 21 data points for both B6 and D2 AHRs were fitted to the 4-parameter function $f(x) = (\max - \min)/[1+ (x/i)^s] + \min$. (B) BNF dose–response curves for B6, D2, and eight B6–D2 chimeric AHRs. These experiments were repeated three times with comparable results; data from one representative experiment are shown. Curve fits were completed, as described above, using the data points shown.

Table 2. Median effective concentration (EC_{50}) ± SD of β-naphthoflavone induction of B6, D2, and chimeric aromatic hydrocarbon receptors (AHR)

AHR	EC_{50} (nM)
B6	18 ± 4
R	14 ± 2
NMR	9 ± 2*
NM	11 ± 2*
PNMR	10 ± 7*
P	13 ± 4
VPNM	430 ± 97*
VP	420 ± 57*
V	330 ± 45*
D2	260 ± 23*

Abbreviations: B6, C57BL/6; D2, DBA/2; SD, standard deviation. Results from three independent dose–response experiments were combined and fitted to a four-parameter function $f(x) = (\max - \min)/[1+ (x/i)^s] + \min$. The EC_{50} and its SD were determined by nonlinear regression.
*Denotes those EC_{50} values that are statistically significantly different from that of the B6 AHR ($p<0.05$).

to contribute greater than twofold to receptor affinity, the opal mutation contributes two- to threefold, and the A375V change contributes four- to sixfold to the differences in AHR affinity (*9,15*). It is therefore very likely that the human *AHR* polymorphism will be made up of at least a dozen, and probably many more, amino acid differences reflecting the variability in ligand affinity.

In this report, we have shown that a yeast-two hybrid assay can readily determine phenotypic differences observed between the B6 and D2 mouse AHR proteins, which leads us to propose that this system might be applicable to the analysis of large numbers of anticipated differences in human AHR proteins. The experiments reported herein only assessed ligand-binding and dimerization properties, and it is possible that functional polymorphisms in a human population may include other steps of the AHR signaling pathway (*5*). Expanding the yeast two-hybrid assay to include a reporter gene that responds to the transactivating activity of AHR/ARNT complexes (*39*) may provide a unique opportunity to identify additional steps in the AHR activation pathway that could be altered and might thus be reflected in the well-documented studies about human variation in CYP1A1 inducibility and AHR affinity.

Our results demonstrate the utility of the oligonucleotide hybridization screening approach for identification of the mouse *Ahr* genotype and of a yeast two-hybrid assay for quantification of the AHR phenotype. Used together, these two methods constitute a powerful novel approach to analyze the role that human *AHR* polymorphisms might play in environmentally related diseases caused by AHR ligands such as dioxin and BaP.

References and Notes

1. ATSDR. Toxicological Profile for Polycyclic Aromatic Hydrocarbons. Atlanta, GA:Agency for Toxic Substances and Disease Registry, 1995.
2. Birnbaum LS. The mechanism of dioxin toxicity: relationship to risk assessment. Environ Health Perspect 102(suppl 9):157–167 (1994).
3. ATSDR. Toxicological Profile for Chlorinated Dibenzo-*p*-dioxins. Atlanta, GA:Agency for Toxic Substances and Disease Registry, 1997.
4. Poland A, Knutson JC. 2,3,7,8,-Tetrachlorodibenzo-*p*-dioxin and related halogenated aromatic hydrocarbons: examination of the mechanisms of toxicity. Annu Rev Pharmacol Toxicol 22:517–554 (1982).
5. Swanson HI, Bradfield CA. The AH receptor: genetics, structure and function. Pharmacogenetics 3:213–230 (1993).
6. Poland A, Glover E, Robinson JR, Nebert DW. Genetic expression of aryl hydrocarbon hydroxylase activity. Induction of monooxigenase activities and cytochrome P_1-450 formation by 2,3,7,8-tetrachlorodibenzo-*p*-dioxin in mice genetically "nonresponsive" to other aromatic hydrocarbons. J Biol Chem 249:5599–5606 (1974).
7. Poland A, Glover E, Kende AS. Stereospecific, high affinity binding of 2,3,7,8-tetrachlorodibenzo-*p*-dioxin by hepatic cytosol. Evidence that the binding species is receptor for induction of aryl hydrocarbon hydroxylase. J Biol Chem 251:4936–4946 (1976).
8. Nebert DW. The *Ah* locus: genetic differences in toxicity, cancer, mutation, and birth defects. Crit Rev Toxicol 20:153–174 (1989).
9. Poland A, Palen D, Glover E. Analysis of the four alleles of the murine aryl hydrocarbon receptor. Mol Pharmacol 46:915–921 (1994).
10. Burbach KM, Poland A, Bradfield CA. Cloning of the Ah receptor cDNA reveals a distinctive ligand-activated transcription factor. Proc Natl Acad Sci USA 89: 8185–8189 (1992).
11. Ema M, Sogawa K, Watanabe N, Chujoh Y, Matsushita N, Gotoh O, Funae Y, Fujii-Kuriyama Y. cDNA cloning and structure of mouse putative Ah receptor. Biochem Biophys Res Commun 184:246–253 (1992).
12. Chang C, Smith DR, Prasad VS, Sidman CL, Nebert DW, Puga A. Ten nucleotide differences, five of which cause amino acid changes, are associated with the Ah receptor locus polymorphism of C57BL/6 and DBA/2 mice. Pharmacogenetics 3:312–321 (1993).
13. Schmidt JV, Carver LA, Bradfield CA. Molecular characterization of the murine *Ahr* gene. J Biol Chem 268:22203–22209 (1993).
14. Mimura J, Ema M, Sogawa K, Ikawa S, Fujii-Kuriyama Y. A complete structure of the mouse Ah receptor gene. Pharmacogenetics 4: 349–354 (1994).
15. Ema M, Ohe N, Suzuki M, Mimura J, Sogawa K, Ikawa S, Fujii-Kuriyama Y. Dioxin-binding activities of polymorphic forms of mouse and human aryl hydrocarbon receptors. J Biol Chem 269:27337–27343 (1994).
16. Poland A, Glover E, Taylor BA. The murine Ah locus: a new allele and mapping to chromosome 12. Mol Pharmacol 32:471–478 (1987).
17. Okey AB, Vella LM, Harper PA. Detection and characterization of a low affinity form of cytosolic Ah receptor in livers of mice nonresponsive to induction of cytochrome P_1-450 by 3-methylcholanthrene. Mol Pharmacol 35:823–830 (1989).
18. Harper PA, Golas CL, Okey AB. Ah receptor in mice genetically "nonresponsive" for cytochrome P450 1A1 induction: cytosolic Ah receptor, transformation to the nuclear binding state, and induction of aryl hydrocarbon hydroxylase by halogenated and nonhalogenated aromatic hydrocarbons in embryonic tissues and cells. Mol Pharmacol 40:818–826 (1991).
19. Niwa A, Kumaki K, Nebert DW. Induction of aryl hydrocarbon hydroxylase activity in various cell cultures by 2,3,7,8-tetrachlorodibenzo-*p*-dioxin. Mol Pharmacol 11:399–408 (1975).
20. Kellermann G, Shaw CR, Luyten-Kellerman M. Aryl hydrocarbon hydroxylase inducibility and bronchogenic carcinoma. N Engl J Med 289:934–937 (1973).
21. Gahmberg CG, Sekki A, Kosunen TU, Holsti LR, Makela O. Induction of aryl hydrocarbon hydroxylase activity and pulmonary carcinoma. Int J Cancer 23:302–305 (1979).
22. Micka J, Milatovich A, Menon A, Grabowski GA, Puga A, Nebert DW. Human Ah receptor (*AHR*) gene: localization to 7p15 and suggestive correlation of polymorphism with CYP1A1 inducibility. Pharmacogenetics 7:95–101 (1997).
23. Puga A, Nebert DW, McKinnon RA, Menon AG. Genetic polymorphisms in human drug-metabolizing enzymes: potential uses of reverse genetics to identify genes of toxicological relevance. Crit Rev Toxicol 27:199–222 (1997).
24. Okey AB, Manchester DK, Feeley MM, Grant DL, Gilman A. Ah receptor characterization in human placenta samples. Organohalogen Compounds 25:177–184 (1995).
25. Okey AB, Giannone JV, Smart W, Wong JMY, Manchester DK, Parker NB, Feeley MM, Grant DL, Gilman A. Binding of 2,3,7,8-tetrachlorodibenzo-*p*-dioxin to Ah receptor in placentas from normal versus abnormal pregnancy outcomes. Chemosphere 34:1535–1547 (1997).
26. Harper PA, Golas CL, Okey AB. Characterization of the Ah receptor and aryl hydrocarbon hydroxylase induction by 2,3,7,8-tetrachlorodibenzo-*p*-dioxin and benzo[*a*]anthracene in the human A431 squamous cell carcinoma line. Cancer Res 48:2388–2395 (1988).
27. Dolwick KM, Schmidt JV, Carver LA, Swanson HI, Bradfield CA. Cloning and expression of a human Ah receptor cDNA. Mol Pharmacol 44:911–917 (1993).
28. Takahashi Y, Itoh S, Shimojima T, Kamataki T. Characterization of Ah receptor promoter in human liver cell line, HepG2. Pharmacogenetics 4:219–222 (1994).
29. Kawajiri K, Watanabe J, Eguchi H, Nakachi K, Kiyohara C, Hayashi S. Polymorphisms of human Ah receptor gene are not involved in lung cancer. Pharmacogenetics 5:151–158 (1995).
30. Wetmur JG. DNA probes: applications of the principles of nucleic acid hybridization. Crit Rev Biochem Mol Biol 26:227–259 (1991).
31. Southern EM. DNA chips: analyzing sequence by hybridization to oligonucleotides on a large scale. Trends Genet 12:110–115 (1996).
32. Matsushita N, Sogawa K, Ema M, Yoshida A, Fujii-Kuriyama Y. A factor binding to the xenobiotic responsive element (XRE) of P450 1A1 gene consists of at least two helix-loop-helix proteins, Ah receptor and Arnt. J Biol Chem 268:21002–21006 (1993).
33. Mason GG, Witte AM, Whitelaw ML, Antonsson C, McGuire J, Wilhelmsson A, Poellinger L, Gustafsson JA. Purification of the DNA-binding form of dioxin receptor. Role of the Arnt cofactor in regulation of dioxin receptor function. J Biol Chem 269:4438–4449 (1994).
34. Dzeletovic N, McGuire J, Daujat M, Tholander J, Ema M, Fujii-Kuriyama Y, Bergman J, Maurel P, Poellinger L. Regulation of dioxin receptor function by omeprazole. J Biol Chem 272:12705–12713 (1997).
35. Chang C, Puga A. Constitutive activation of the aromatic hydrocarbon receptor. Mol Cell Biol 18:525–535 (1998).
36. Kouri RE, McKinney CE, Slomiany DJ, Snodgrass DR, Wray NP, McLemore TL. Positive correlation between high aryl hydrocarbon hydroxylase activity and primary lung cancer as analyzed in cryopreserved lymphocytes. Cancer Res 42: 5030–5037 (1982).
37. Nebert DW, Puga A, Vasiliou V. Role of the Ah receptor and the dioxin-inducible [*Ah*] gene battery in toxicity, cancer, and signal transduction. Ann NY Acad Sci 685:624–640 (1993).
38. Heuvel JPV, Clark GC, Thompson CL, McCoy Z, Miller CR, Lucier GW, Bell DA. CYP1A1 mRNA levels as a human exposure biomarker: use of quantitative polymerase chain reaction to measure CYP1A1 expression in human peripheral blood lymphocytes. Carcinogenesis 14:2003–2006 (1993).
39. Carver LA, Jackiw V, Bradfield CA. The 90-kDa heat shock protein is essential for Ah receptor signaling in a yeast expression system. J Biol Chemistry 269: 30109–30112 (1994).
40. Rowlands JC, Gustafsson JA. Human dioxin receptor chimera transactivation in a yeast model system and studies on receptor agonists and antagonists. Pharmacol Toxicol 76:328–333 (1995).
41. Yamaguchi Y, Kuo MT. Functional analysis of aryl hydrocarbon receptor nuclear translocator interactions with aryl hydrocarbon receptor in the yeast two-hybrid system. Biochem Pharmacol 50:1295–1302 (1995).
42. Conner BJ, Reyes AA, Morin C, Itakura K, Teplitz RL, Wallace RB. Detection of sickle cell β^S-globin allele by hybridization with synthetic oligonucleotides. Proc Natl Acad Sci USA 80:278–282 (1983).
43. Bugawan TL, Apple R, Erlich HA. A method for typing polymorphism at the *HLA-A* locus using PCR amplification and immobilized oligonucleotide probes. Tissue Antigens 44:137–147 (1994).
44. Strewing JP, Brody LC, Erdos MR, Kase RG, Giambarresi TR, Smith SA, Collins FS, Tucker MA. Detection of eight *BRCA1* mutations in 10 breast/ovarian cancer families, including 1 family with male breast cancer. Am J Hum Genet 57:1–7 (1995).
45. Hacia JG, Brody LC, Chee MS, Fodor SPA, Collins FS. Detection of heterozygous mutations in *BRCA1* using high density oligonucleotide arrays and two-colour fluorescence analysis. Nature Genet 14:441–447 (1996).
46. Drobyshev A, Mologina N, Shik V, Pobedimskaya D, Yershov G, Mirzabekov A. Sequence analysis by hybridization with oligonucleotide microchip: identification of β-thalassemia mutations. Gene 188:45–52 (1997).